Journal of Solid State Chemistry 182 (2009) 991–994

Contents lists available at ScienceDirect

Journal of Solid State Chemistry

journal homepage: www.elsevier.com/locate/jssc

One-pot synthesis of superacid catalytic material SO_4^{2-}/ZrO_2–SiO_2 with thermostable well-ordered mesoporous structure

Ruifeng Li *, Feng Yu, Fuxiang Li, Meimei Zhou, Bingshe Xu, Kechang Xie

Institute of Special Chemicals, Key Laboratory of Coal Science and Technology MOE, Taiyuan University of Technology, Taiyuan 030024, China

ARTICLE INFO

Article history:
Received 31 January 2008
Received in revised form
7 April 2008
Accepted 13 April 2008
Available online 20 April 2008

Keywords:
Mesoporous catalyst
Superacid
One-pot synthesis
Isomerization
Tetragonal zirconia

ABSTRACT

A superacid mesostructured catalyst was directly synthesized by adding sulfuric acid to mesoporous zirconia–silica synthesis mixtures, and was characterized by HRTEM, XRD, UV–Vis, nitrogen sorption, NH_3–TPD, and Pyridine–FTIR. The XRD patterns and electron diffraction micrographs of the calcined samples showed the ordered mesoporous structure and tetragonal crystalline in frameworks. The ammonia TPD, pyridine *in situ* FTIR, and paraffin isomerization illustrated a new acidic property of the samples. The synthesis of the mesoporous materials, which have stable crystalline frameworks, high surface area, and strong acidity, is very likely to have important technological implications for catalytic reactions of large molecules.

1. Introduction

Since ordered mesoporous aluminosilicate materials, such as MCM41s, were synthesized in 1992 [1], mesoporous molecular sieves have attracted strong interest because of their potential applications in advanced catalytically materials and adsorbents. The crucial problem is that the mesoporous aluminosilicate represents poor hydrothermal stability, either in stream or in hot water. As a result, the application of new materials has been limited [2]. Subsequently, researchers used a triblock copolymer to organize the structure of a polymeric silica precursor template to form new mesoporous silica denoted SBA-15 with periodic 5–30 nm pores. SBA-15 has more regular structure and thicker walls than MCM-41, resulting in higher stability, but low catalytic activity due to its pure silica frameworks [3]. Compared with crystalline zeolites, mesoporous materials exhibited insufficient hydrothermal stability and acidity. This difference draws many researchers to improve the framework crystallinity and acidity for practical applications. Recently, significant progresses in developing new mesoporous structures have been made [4,5–8]. However, properties of the parent mesostructured materials, including so-called mesoporous zeolites, were not comparable with that of crystalline zeolites used in the industry [9].

While various attempts have been reported to improve framework crystallinity of the mesoporous aluminosilicate materials, the relatively low acidity, unsatisfactory pore structure, and thermal stability have not been completely resolved. On the other hand, the mesoporous materials containing zirconium have received considerable attention in heterogeneous catalysis because of their potential acid properties [10–12]. The mesoporous structure of these materials is unstable in thermal treatment and will collapse when at temperatures above 600 °C. Adding sulfate anions to the material at the precipitation stage or through post-treatment of the formed mesoporous phase using sulfuric acid or ammonium sulfate plays an important role for stabilizing the mesoporous structure of ZrO_2 and enhancing the acidic properties. Several practices have succeeded in introducing zirconium into the framework of molecular sieves during synthesis, but the material has a ratio of Zr/Si lower than 0.025 [13]. Thermally stable mesoporous materials based on silica-stabilized zirconia were synthesized in two steps using hexadecyl trimethyl ammonium bromide as a template. These silica-stabilized materials have still an amorphous phase up to 600 °C, in which the strength of most acid sites is similar to that in conventional SO_4^{2-}/ZrO_2. This process partly improves acidity and/or hydrothermal stability [14]. Recently, we reported a new strategy to directly synthesis Zr-SBA-15 using a triblock copolymer and hexadecyl trimethyl ammonium bromide (CTAB) as co-templates, and then sulfated to obtain a mesostructured SO_4^{2-}/ZrO_2 material with high surface area and strong acidity used in paraffin isomerization [15]. Herein, we report a direct synthesis route to mesoporous superacid catalysts SO_4^{2-}/ZrO_2–SiO_2 (denoted as MSC_x, here x is Zr/Si ratio) with ordered mesoporous structure and crystalline frameworks by one-pot method.

* Corresponding author. Fax: +86 351 6010121.
E-mail address: rfli@tyut.edu.cn (R. Li).

0022-4596/$ - see front matter © 2009 Elsevier Inc. All rights reserved.
doi:10.1016/j.jssc.2008.04.009

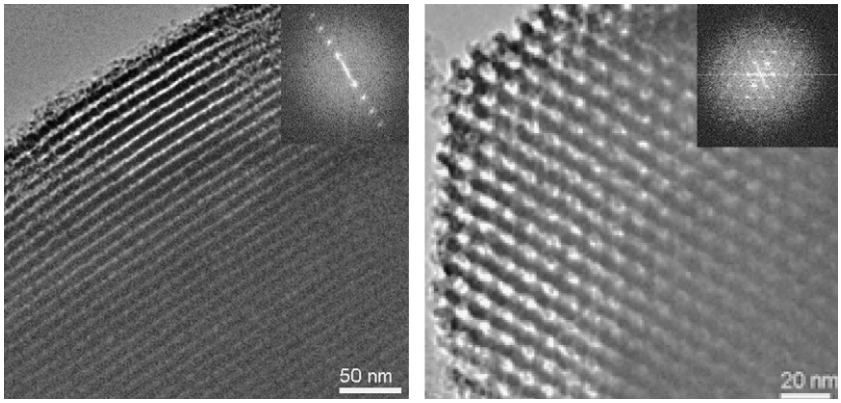

Fig. 1. TEM images of the calcined mesoporous catalyst MSC_x ($x = 1.1$). Insets: the corresponding electron diffraction pattern.

2. Experimental

In a typical synthesis, 15 ml of alcohol solution containing 1.63 g CTAB were fully mixed with 40 ml of alcohol solution containing 4.4 g $Zr(NO_3)_4 \cdot 3H_2O$ and then transferred into Teflon-lined autoclave and preheated at 110 °C for 3.5 h to obtain sample-I. The 20 ml of 1 mol/l H_2SO_4 solution were mixed with 20 ml of 2 mol/l HCl solution containing 1 g triblock poly(ethylene oxide)–poly(propylene oxide)–poly(ethylene oxide) (EO_{20}–PO_{70}–EO_{20}, P_{123}, Aldrich), 2.3 ml of tetraethyl orthosilicate (TEOS) were added in the mixture and stirred for 3 h at 40 °C to obtain sample-II. Sample-I was mixed with sample-II under stirring. The final mixture was stirred continuously for another 3 h and then transferred into Teflon-lined autoclave at 100 °C for 48 h. The as-synthesized solid was filtered, washed with distilled water and dried, and calcined in air flow at 600 °C for 3 h to obtain MSC. The MSC_x ($x = 0.1$–3.0) were synthesized in the same processing and characterized by the techniques such as high-resolution transmission electron microscopy (HRTEM), field emission scanning electron microscopy (FESEM), X-ray powder diffraction (XRD), UV–Vis, N_2 adsorption isotherm, and the temperature-programmed desorption of ammonia.

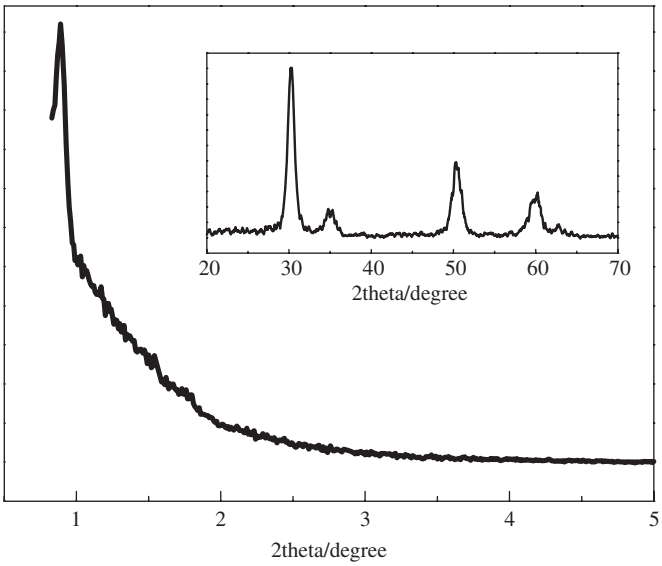

Fig. 2. XRD pattern of the calcined mesoporous catalyst MSC_x ($x = 1.1$).

3. Results and discussion

The HRTEM images of the calcined MSC sample (Fig. 1) show well-ordered hexagonal arrays of mesopores with one-dimensional channels and unambiguously confirm that the hexagonal pore structure of the SBA-15 was retained. The corresponding electron diffraction patterns (insets of Fig. 1) indicate that the final product was a mesoporous material with a polycrystalline framework. During the calcination, tetragonal ZrO_2 began to take into form, and at the same time it incorporated and coordinated in the silica framework. The existence of tetrahedral ZrO_2 in silica framework was suggested by ^{29}Si NMR spectra [15]. A well-ordered mesoporous material with partial crystalline frameworks is well supported by a small-angel XRD peak at $2\theta = 0.9^\circ$ and the wide-angel XRD peaks corresponding to the ZrO_2 tetragonal structure (inset in Fig. 2). One diffraction peak in the low angle region ($2\theta \leqslant 5$) is visible indicating that MSC has a long-range hexagonal ordering. Bulk MSC shows the pure tetragonal phase of zirconia in the ordinary region ($2\theta = 30$–50) rather than a monoclinic zirconia phase. As indicated by SEM (not shown) and HRTEM images, no aggregated ZrO_2 particles can be observed. The corresponding electron diffraction (inset in Fig. 1) indicated that the final product was a mesoporous material with a crystalline framework. The porosity of the MSC materials was studied by

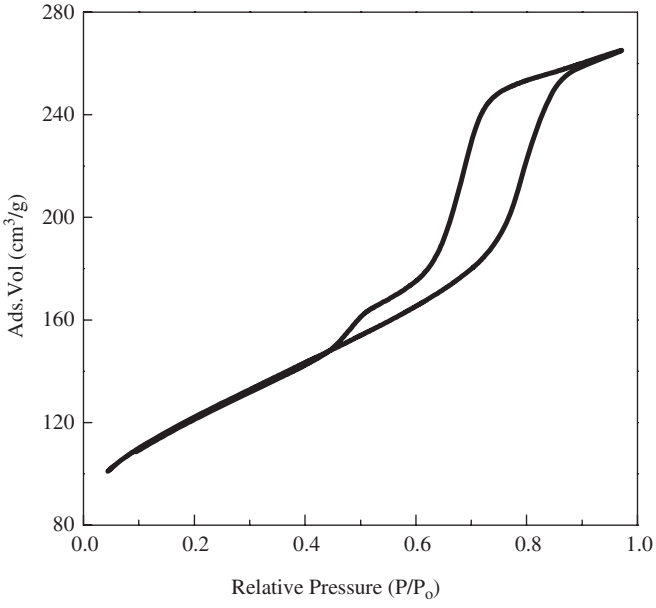

Fig. 3. N_2 adsorption isotherm of the calcined mesoporous MSC_x ($x = 1.1$).

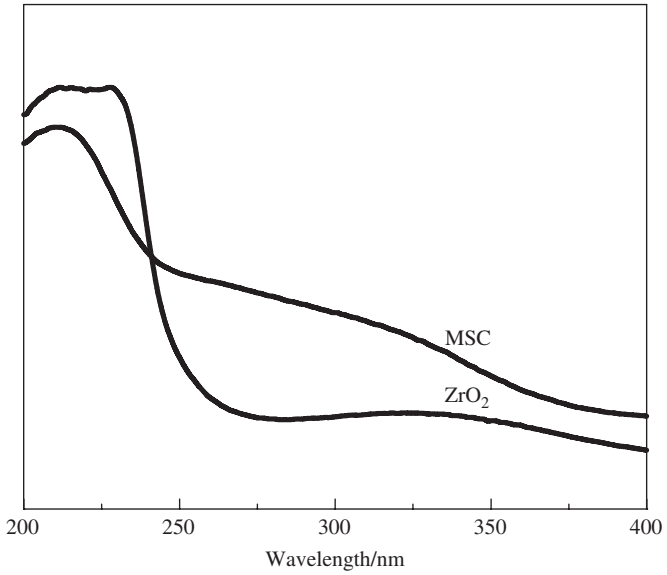

Fig. 4. UV–Vis spectra of the calcined mesoporous catalyst MSC_x ($x = 1.1$) and pure ZrO_2.

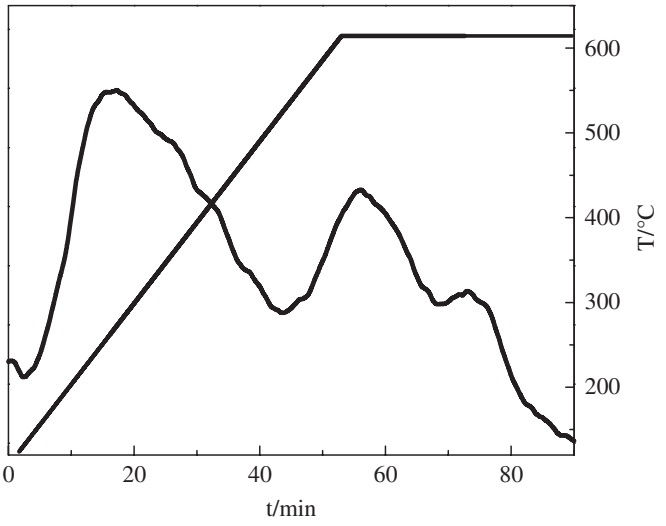

Fig. 5. The temperature-programmed desorption of ammonia on the calcined mesoporous catalyst MSC_x ($x = 1.1$).

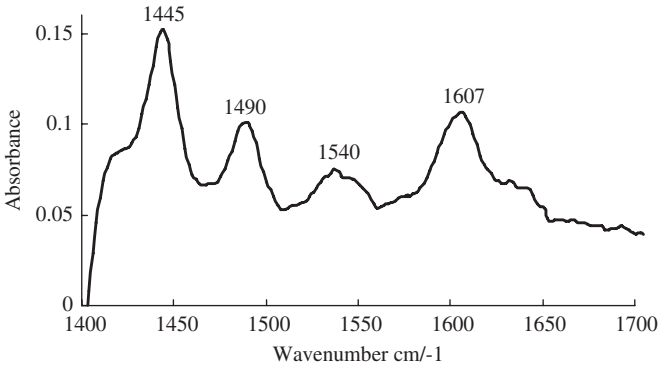

Fig. 6. *In situ* FTIR spectrum of pyridine adsorption in the sample MSC_x ($x = 1.1$) at 150 °C.

measuring gas N_2 adsorption at 77 K. A type-IV isotherm is showed in N_2 adsorption–desorption on a typical sample (Fig. 3). The location of the hysteresis loops in the interval of P/P_0 ranging from 0.45 to 0.9, the steep increase in the adsorption value in this pressure range, together with the fact that the adsorption and desorption branches are parallel to each other suggest that the sample possesses a highly ordered framework with cylindrical mesoporous channels. This behavior is indicative of a uniform mesopore size distribution, which is filled spontaneously due to capillary condensation in the MSC materials. The pore size distributions have been determined by referring to the BJH model applied to desorption isotherm branch. The mesopore diameter is centered at 3.8 nm, in agreement with the result of HRTEM. The surface area is more than 300 m^2/g. With increase of the Zr/Si ratio, the surface area of the calcined samples varies from 600 ($x = 0.3$) to 200 m^2/g ($x = 3.0$). The UV–Vis DRS spectra of the calcined samples are provided in Fig. 4. Two broad bands centered at 210 and 230 nm are shown in spectra of zirconia, corresponding to the characteristic peaks of *t*-ZrO_2 and *m*-ZrO_2 phases [16], in line with the interpretation of the XRD patterns shown in Fig. 2. The absorption in the region 250–350 nm is resulted from defects in zirconia [17]. The spectra of the MSC sample are dominated by a strong adsorption whose maximum is near 210 nm, previously assigned to an $O_4^+ \rightarrow ZrO_4^+$ charge transfer transition of tetrahedrally coordinated Zr in the silicalite framework, typical of Zr silicalite. The peak at 230 nm corresponding to octahedral zirconium species disappeared [16,17]. The surface acidity of the samples is investigated by NH_3–TPD method and *in situ* pyridine adsorption FTIR spectra. The introduction of sulfate ion must have stabilized the tetragonal phase of the zirconia, which is an ideal phase for the exhibiting superacidity for sulfated zirconia [18]. A typical NH_3–TPD profile of a typical sample after calcination at 600 °C is shown in Fig. 5. Three desorption peaks occur at low temperature around 265 °C and high temperature at 600 °C. The first group of peaks (120–450 °C) suggests that MSC possesses a large number of acid sites with intermediate and strong acid strength. The peak at 600 °C corresponding to very strong acid strengths implies superacidic centers for zirconia-based catalysts [19]. The super-acidic sites of $MSC_{1.1}$ are 36.6% of the total acid sites (0.87 mmol/g). To differentiate Brønsted and Lewis sites, basic molecules with relatively high acid strengths are used, with pyridine being the most frequently used base. The frequency of the ring deformation vibration allows to differentiate whether pyridine is adsorbed on Brønsted acid sites in the form of pyridinium ions (1544 cm^{-1}) or coordinatively adsorbed on Lewis acid sites (1455–1442 cm^{-1}). The higher the latter wavenumber is, the stronger the interaction with a Lewis acid site. The intensive band at 1490 cm^{-1} results from both contributions, i.e. Brønsted and Lewis sites [20]. Fig. 6 illustrates the FTIR spectra of pyridine adsorption over the sample at 150 °C, pyridinium ions (pyridine–Brønsted acid site complex) are indicated by IR vibrations at 1610, 1540, and 1490 cm^{-1}, as well as covalently bound pyridine (pyridine–Lewis acid site complex) at 1490 and 1445 cm^{-1}. The strength of Lewis acid sites is stronger than that of Brønsted ones.

The acid sites in the surface of catalyst may be characterized by qualifying the predominant acid-type species present, usually expressed as the *B*/*L* ratio and calculated from the IR peak intensities of the pyridine–Brønsted acid site complex at 1540 cm^{-1} and pyridine–Lewis acid site complex at 1445 cm^{-1}. For samples SO_4^{2-}/ZrO_2–SiO_2 (MSC_x) synthesized in the present work, the *L*/*B* ratios are more than 1.0 at adsorption temperature of 150 °C. With increase of Zr/Si ratio in the samples, the *L*/*B* ratio decreases. As the pyridine desorption temperature increases from 150 to 350 °C, the *L*/*B* ratio increases. High surface area sulfated zirconia catalysts possessed *n*-butane isomerization activity superior to conventional ambient preparations [21]. The catalytic properties of the MSC_x samples were also studied in the catalytic conversion of *n*-pentane at ambient temperature. The

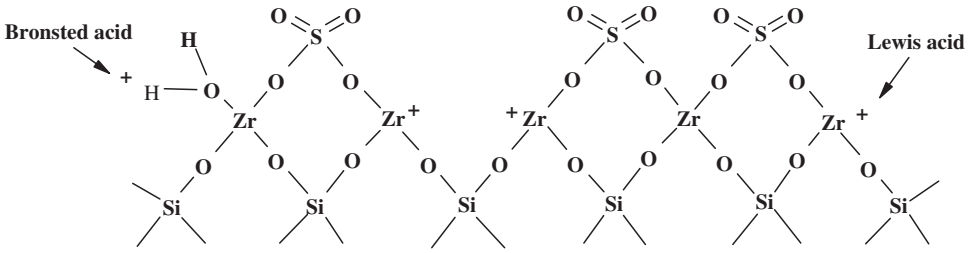

Scheme 1. Proposed surface model and superacidic species.

results showed that the catalysts have near 100% selectivity of isoparaffin under the conversion of over 50% on the sample $MSC_{1.1}$ in the steady-time for 3 days.

The above results have revealed the special properties of the catalysts, in which the key element is more notably that these materials used as catalysts have high thermo- and hydrothermostability, and regenerated capability, besides their unique surface acidity (the prolific Lewis acid sites and real superacid strength). The high stability lies undoubtedly on the stable structure of the mesporous materials because of the construction of the crystalline ZrO_2 with the tetrahedral SiO_2 in the wall framework. The stable surface acidity discloses probably a novel surface structure formed from ZrO_2 and SiO_2 with SO_4^{2-}. A logical surface structural model is suggested (see Scheme 1); however, the reaction mechanism is yet undiscovered. The substitution of Si–O– by Zr–O– ligands significantly arises on the surface and the crystalline tetragonal zirconia appears after the calcinations at 600 °C, as confirmed by XRD. The surface defect (from UV–Vis results) increases the amount of Lewis acid sites, the Si–O–Zr–O–Zr–O–Si construction improves the stability of Zr–O–S linkage structure and the dispersivity of the surface acid sites, resulting in its stable catalysis of isomerization [22]. In the surface structure of the catalyst, with increase of Zr/Si ratio, the surface defect decreases and so the *L*/*B* ratio decreases (corresponding to the forenamed pyridine–FTIR results).

4. Conclusions

Conclusively, a novel mesoporous solid acid catalytic material MSC was synthesized using one-pot method. The material possesses superior activity, stability, and high surface area and ordered mesoporosity. Zirconia in MSC materials is tetragonal crystalline. The nature of acid sites present on the catalytic materials is Lewis and Brønsted type, and the relative strength of Lewis and Brønsted acid sites can be controlled. The isomerization of *n*-pentane in the ambient temperature indicates the material's large strong acidity performance. The mesoporous structure with strong acidity can be a remarkable benefit for catalytic reactions involving large organic molecules. The synthesis principle developed in the present work may set up a bridge between conventional sulfated zirconia and amorphous mesoporous alumino- or silicates, by which metal-doped mesoprous aluminosilicates could be prepared.

Acknowledgments

Author R. Li thanks Professor E.E. Wolf for his valuable advice and correction. Financial support of this work by the Natural Science Foundation of China (NSFC, No. 50772070) and Shanxi Scientific Research Foundation for the Returned Overseas Chinese is gratefully acknowledged.

References

[1] C.T. Kresge, M.E. Leonowicz, W.J. Roth, J.C. Varuli, J.S. Beck, Nature 359 (1992) 710–712.
[2] A. Corma, Chem. Rev. 97 (1997) 2373–2419.
[3] D. Zhao, J. Feng, Q. Huo, N. Melossh, G.H. Fredrickson, B.F. Chmelka, G.D. Stucky, Science 279 (1998) 548–552.
[4] M.A. Carreon, V.V. Guliants, Eur. J. Inorg. Chem. 2005 (2005) 27–43.
[5] Y. Liu, W. Zang, T.J. Pinnavia, Angew. Chem. Int. Ed. 40 (2001) 1255–1258.
[6] T. Do, A. Nossov, M. Springuel-Huet, C. Schneider, J.L. Bretherton, C.A. Fyfe, S. Kaliaguine, J. Am. Chem. Soc. 126 (2004) 14324–14325.
[7] I.C. Sung, D.C. Sung, H.K. Jong, J.K. Geon, Adv. Funct. Mater. 14 (2004) 49–54.
[8] Y. Fang, H. Hu, J. Am. Chem. Soc. 128 (2006) 10636–10637.
[9] C.H. Christensen, K. Johannsen, I. Schmidt, J. Am. Chem. Soc. 125 (2003) 13370–13371.
[10] M.V. Landau, L. Titelman, L. Vradman, P. Wilson, Chem. Commun. (2003) 594–595.
[11] Y. Wang, K.Y. Lee, S. Choi, J. Liu, L.Q. Wang, C.H.F. Peden, Green Chem. 9 (2007) 540–544.
[12] Q.-H. Xia, K. Hidajat, S. Kawi, J. Catal. 205 (2002) 318–331.
[13] X.X. Wang, F. Lefebvre, J. Patarin, J.M. Basset, Microporous Mesoporous Mater. 42 (2001) 269–276.
[14] A.V. Ivanov, S.V. Lysenko, S.V. Baranova, A.V. Sungurov, T.N. Zangelov, E.A. Karakhanov, Microporous Mesoporous Mater. 91 (2006) 254–260.
[15] F. Li, F. Yu, Y. Li, R. Li, K. Xie, Microporous Mesoporous Mater. 110 (2007) 250–255.
[16] (a) X. Chen, Y. Ju, C.Y. Mu, J. Phys. Chem. C 111 (2007) 18731–18737;
(b) M. Li, Z. Feng, G. Xiong, P. Ying, Q. Xin, C. Li, J. Phys. Chem. B 105 (2001) 8107–8111.
[17] E. Fernández López, V.S. Escribano, M. Panizza, M. Carnasciali, G. Busca, J. Mater. Chem. 11 (2001) 1891–1897.
[18] G.D. Yadav, A.D. Murkute, Adv. Synth. Catal. 346 (2004) 389–394.
[19] A. Corma, V. Fornès, M.I. Juan-Rajadell, J.M. López Nieto, Appl. Catal. A 116 (1994) 151–163.
[20] R. Buzzoni, S. Bordiga, G. Ricchiardi, C. Lamberti, A. Zecchina, Langmuir 12 (1996) 930–940.
[21] M.A. Risch, E.E. Wolf, Appl. Catal. A 172 (1998) L1–L5.
[22] A. Corma, H. Garcıa, Chem. Rev. 103 (2003) 4307–4365.